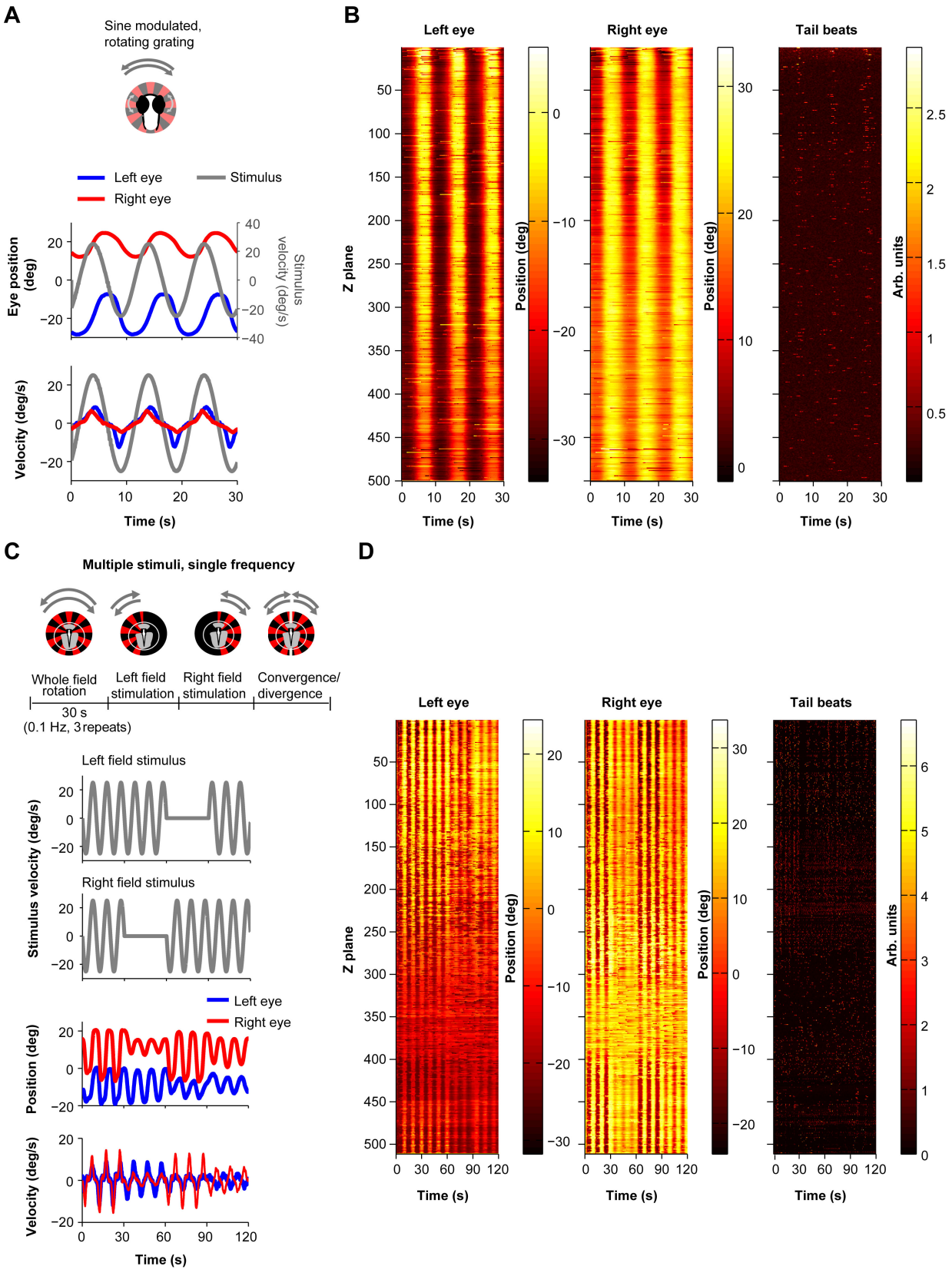

Figure S1
Portugues et al.

Figure S1. Stimuli and behavior (related to Figures 1 and 6)

(A) Optokinetic response (OKR) was elicited by presenting restrained larvae with a rotating pattern of radial stripes with a 45˚ period. *Top,* Stimulus rotation was sinusoidally modulated, with a frequency of 0.1Hz. Larvae tracked the stimulus with their eyes. Mean eye position (center) and eye velocity (bottom) for one fish (data is the same as in Figure 1B). Gray traces show stimulus velocity. For each imaging plane, the stimulus was repeated three times; mean eye data is calculated across imaging planes.

(B) Larvae showed consistent behavior throughout the recording session. Mean subtracted horizontal eye position (left and center) and tail movement (right) for all repetitions. Each row represents a recording plane, with three stimulus repetitions. Eye position was extracted from video recordings, and defined as the angle relative to the midline. Anticlockwise eye positions were defined to be positive. Total imaging time is 4 hours 10 minutes.

(C) Multiple stimuli were used to separate different sensory and motor signals. Top, The stimulus set consisted of a sequence of four stimuli: the standard rotating grating, a rotating grating presented on the left visual field only, a rotating grating presented on the right visual field only, and rotating gratings moving in opposite directions in each eye, to simulate forward and backward motion. Bottom, Traces show the average stimulus velocity on the left and right visual fields, average eye position and average eye velocity across repetitions of a stimulus set. During standard OKR, larvae tracked the stimuli with a conjugate movement of the eyes. When stimuli were presented in an hemifield, the eye ipsilateral to stimulation followed the stimulus while the other eye moved but with smaller amplitude movements. When the direction of movement in the two hemifields was opposite to each other (last stimulus of the stimulus set), larvae followed both stimuli with convergent or divergent movements of the eyes.

(D) Mean subtracted eye (left and center) and tail (right) movement for all repetitions in a recording session. As in (B), note that each row corresponds to an imaging plane, and a stimulus set was repeated three times in each plane. Total imaging time was 17 hours.

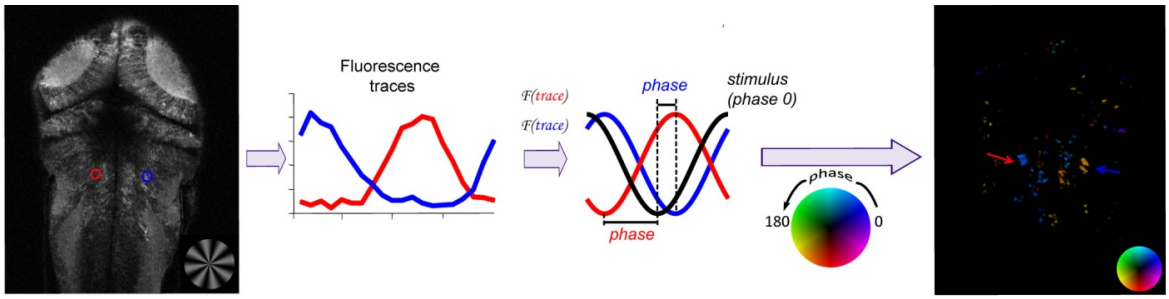

Figure S2

Figure S2. Phase to color transformation (related to Experimental Procedures, and Figures 1 and 4).

Activity modulated at the stimulus frequency can be visualized using phase-color maps. Schematic showing how phases are assigned to two example areas (marked by red and blue circles). For each voxel, or ROI, we compute the Fourier transform of the average fluorescence trace z-score and extract the response component at the stimulus frequency. The phase of this component is used to select a color from a circular hue saturation value colormap (computed using the Matlab hsv function). The color intensity is selected from the amplitude of this same component, which reflects the relative modulation of fluorescence at the stimulus frequency compared to other frequencies. On the right is shown a voxel-wise color map for this plane in the fish. Arrows point to the areas corresponding to the circular ROIs in the left image.

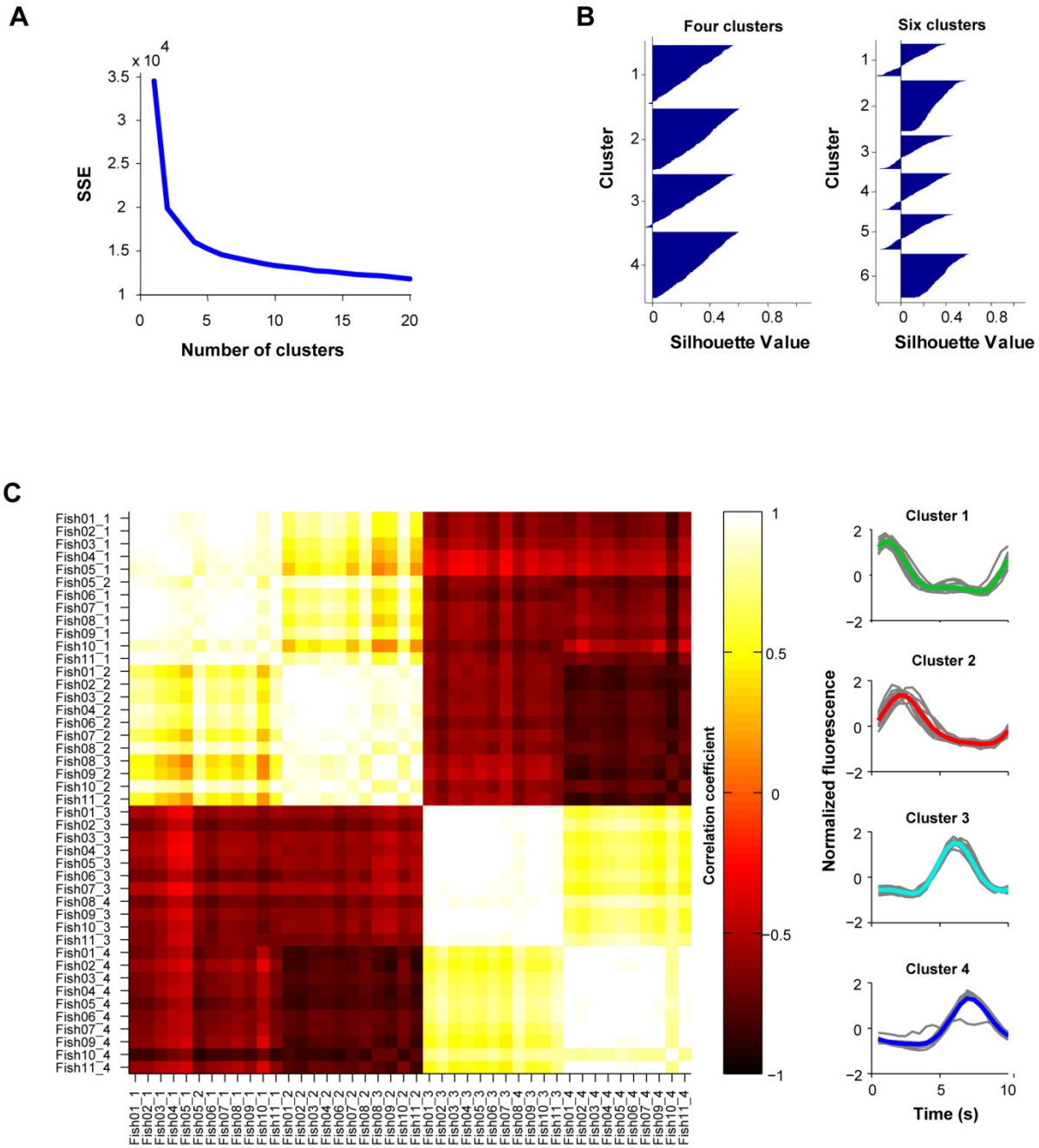
A
x 10^4
SSE
Number of clusters
B
Four clusters
Six clusters
Cluster
Silhouette Value
C
Correlation coefficient
Cluster 1
Cluster 2
Cluster 3
Cluster 4
Normalized fluorescence
Time (s)

Figure S3

Figure S3. Clustering of fluorescence raw traces (related to Figure 2)

(A) Graph of total sum of squared errors (SSE) of within cluster distances (from all individual points to the centroid of their cluster) as a function of *k*, the number of clusters used in the k-means clustering. This graph is monotonically decreasing. We used the elbow method to estimate the number of clusters to use.

(B) Silhouette plots comparing clustering into 4 (*left)* and 6 (*right)* clusters. The silhouette plots for 4 clusters show that clustering into 4 groups matches the data better.

(C) Similar clusters were found in almost all fish that responded to the stimulus. Cluster analysis was applied independently to each of 11 fish that showed consistent behaviour, assigning every ROI to one of four clusters. *Left,* Correlation of the average traces for all clusters, shows that the pooled set of clusters themselves separate into 4 groups, which, with one exception, matches the classification in each single fish. *Right,* average traces across all fish for each of the four clusters, ordered by peak response timing. Compare to Figure 1F.

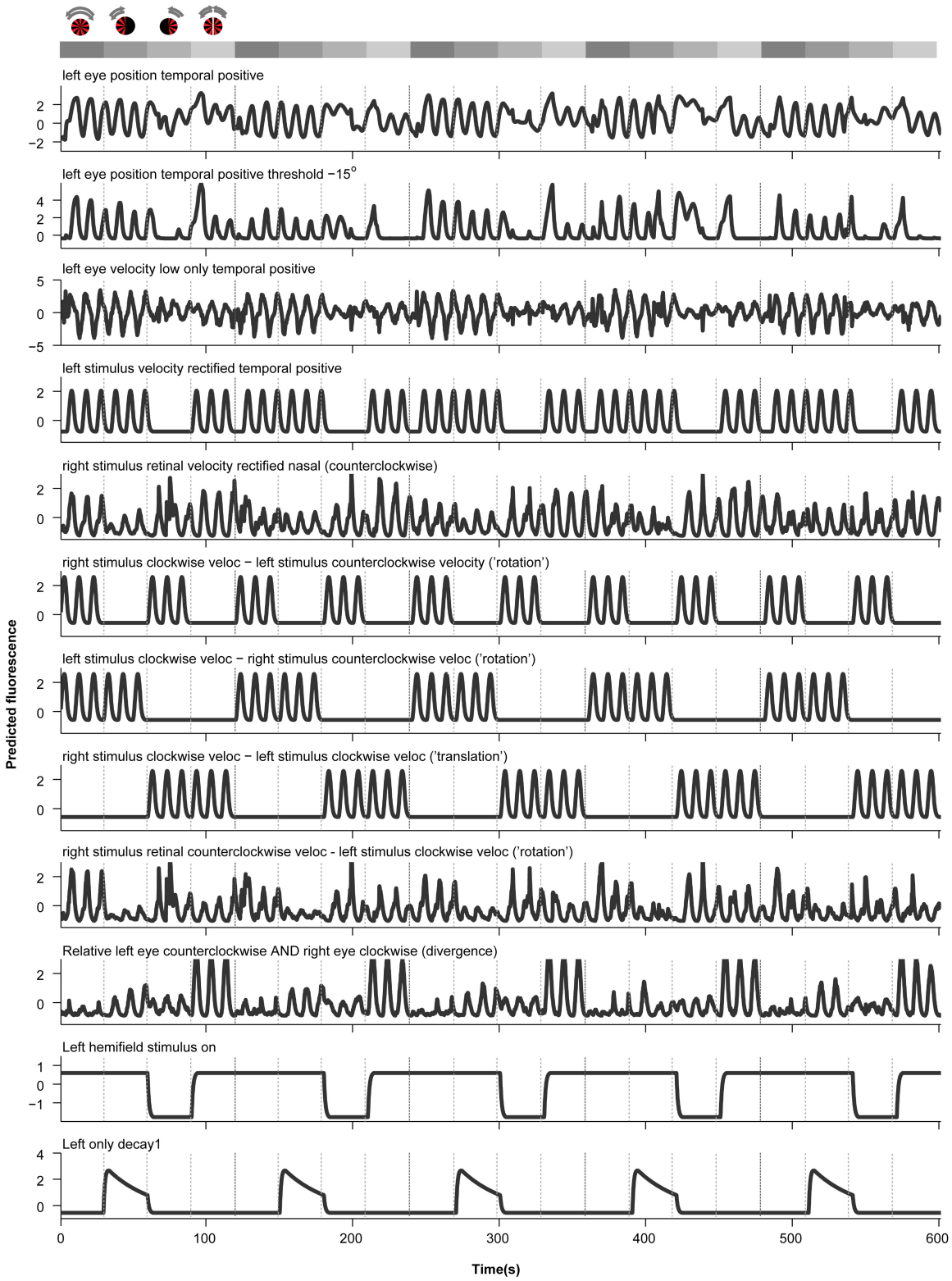

Figure S4
Portugues et al.

Figure S4. Examples of some of the regressors used for correlation analysis (related to Experimental Procedures, and Figures 6-8, S6-S8)

Examples of regressors used for comparison with fluorescence traces. Stimulus and motor variables are convolved with the predicted GCaMP5G response kernel. In addition to the raw variables, simple operations, such as thresholding or adaptation, combinations of multiple variables, rectification, and transformation of motion from visual to retinal coordinates were also tested. A schematic of the four stimuli is shown (see Figures 6 and S1). Gray boxes and dotted lines indicate the duration of each of the four stimuli in all plots.

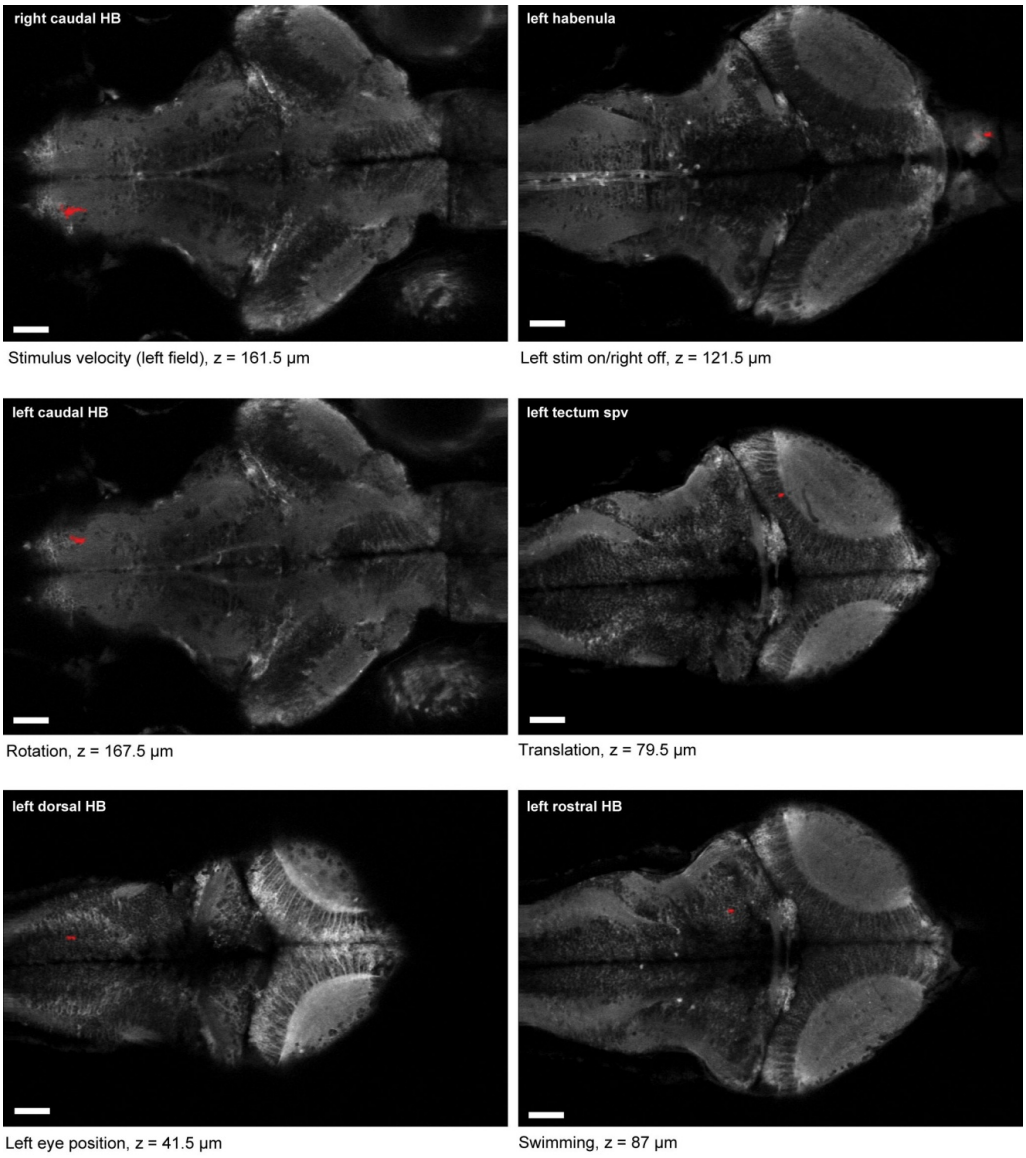

Figure S5

Figure S5. Anatomical localization of ROIs shown in Figure 6 (related to Figure 6)

The ROIs for the example traces in Figure 6 are shown superimposed on the average GCaMP5G fluorescence as anatomical reference. HB: hindbrain; spv: stratum periventriculare. Scale bar 50 µm.

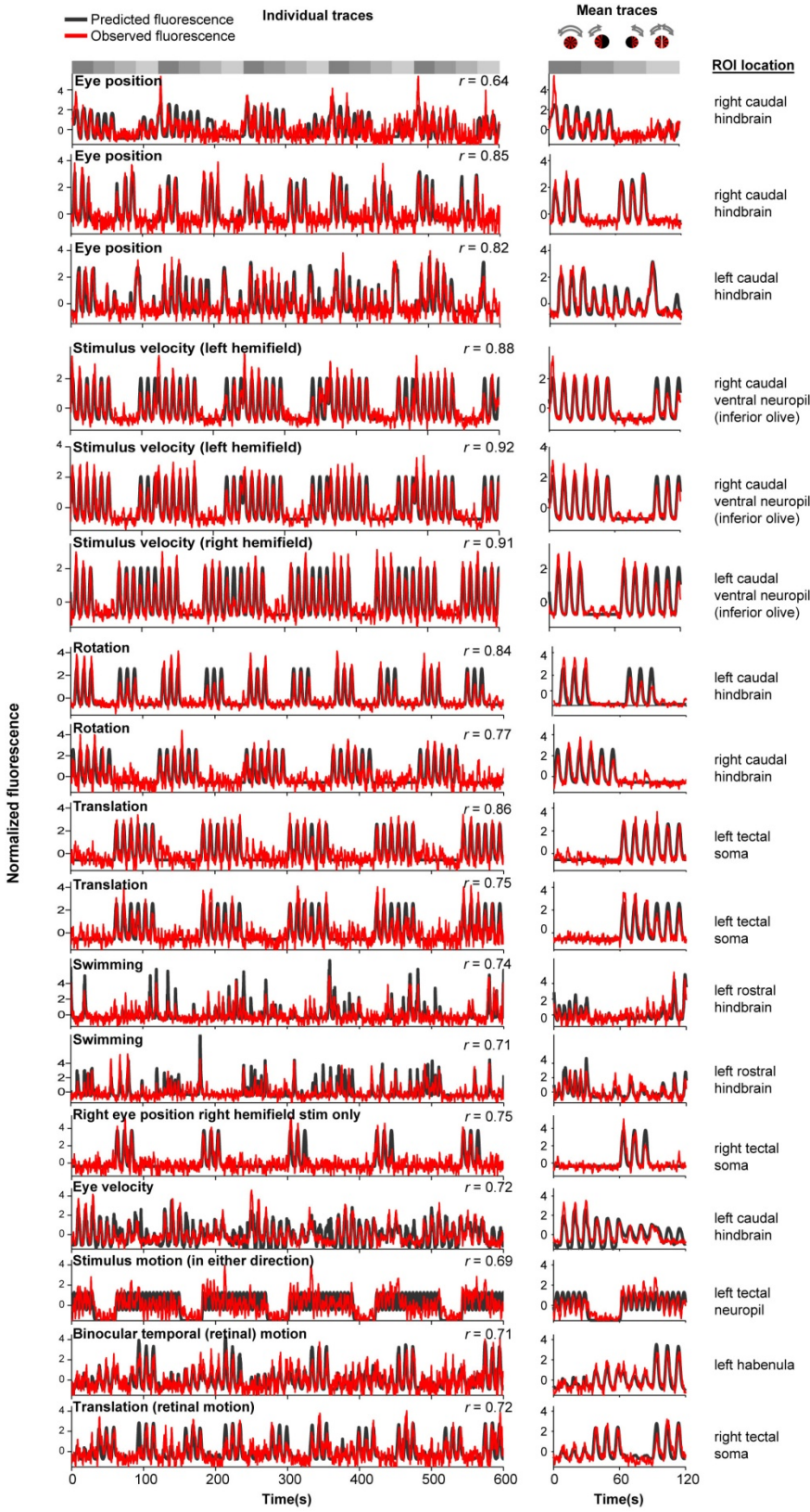
Predicted fluorescence
Observed fluorescence
Individual traces
Mean traces
ROI location
Eye position
r = 0.64
right caudal hindbrain
Eye position
r = 0.85
right caudal hindbrain
Eye position
r = 0.82
left caudal hindbrain
Stimulus velocity (left hemifield)
r = 0.88
right caudal ventral neuropil (inferior olive)
Stimulus velocity (left hemifield)
r = 0.92
right caudal ventral neuropil (inferior olive)
Stimulus velocity (right hemifield)
r = 0.91
left caudal ventral neuropil (inferior olive)
Rotation
r = 0.84
left caudal hindbrain
Rotation
r = 0.77
right caudal hindbrain
Translation
r = 0.86
left tectal soma
Translation
r = 0.75
left tectal soma
Swimming
r = 0.74
left rostral hindbrain
Swimming
r = 0.71
left rostral hindbrain
Right eye position right hemifield stim only
r = 0.75
right tectal soma
Eye velocity
r = 0.72
left caudal hindbrain
Stimulus motion (in either direction)
r = 0.69
left tectal neuropil
Binocular temporal (retinal) motion
r = 0.71
left habenula
Translation (retinal motion)
r = 0.72
right tectal soma
Normalized fluorescence
Time(s)
Time(s)

Figure S6

Figure S6. Further examples of ROIs that correlated with behavioral variables (related to Figure 6)

Further example traces of different ROIs taken from individual whole-brain imaging data sets that best correlated with eye position, stimulus velocity, stimulus rotation, stimulus translation, swimming, as well as variables not shown in Figure 6. *Left*, fluorescence data from the subset of the ROI that intersects each imaging plane (red) and the regressor that best correlates with this trace (black). Each plane contains different numbers of pixels in the ROI, and behavior will vary slightly between planes. *Right*, average fluorescence trace, and average regressor values through the whole ROI. *r*, correlation coefficient between the shown traces. A schematic of the four stimuli is shown above the mean traces (see Figures 6 and S1). Gray boxes and dotted lines indicate the duration of each of the four stimuli in all plots.

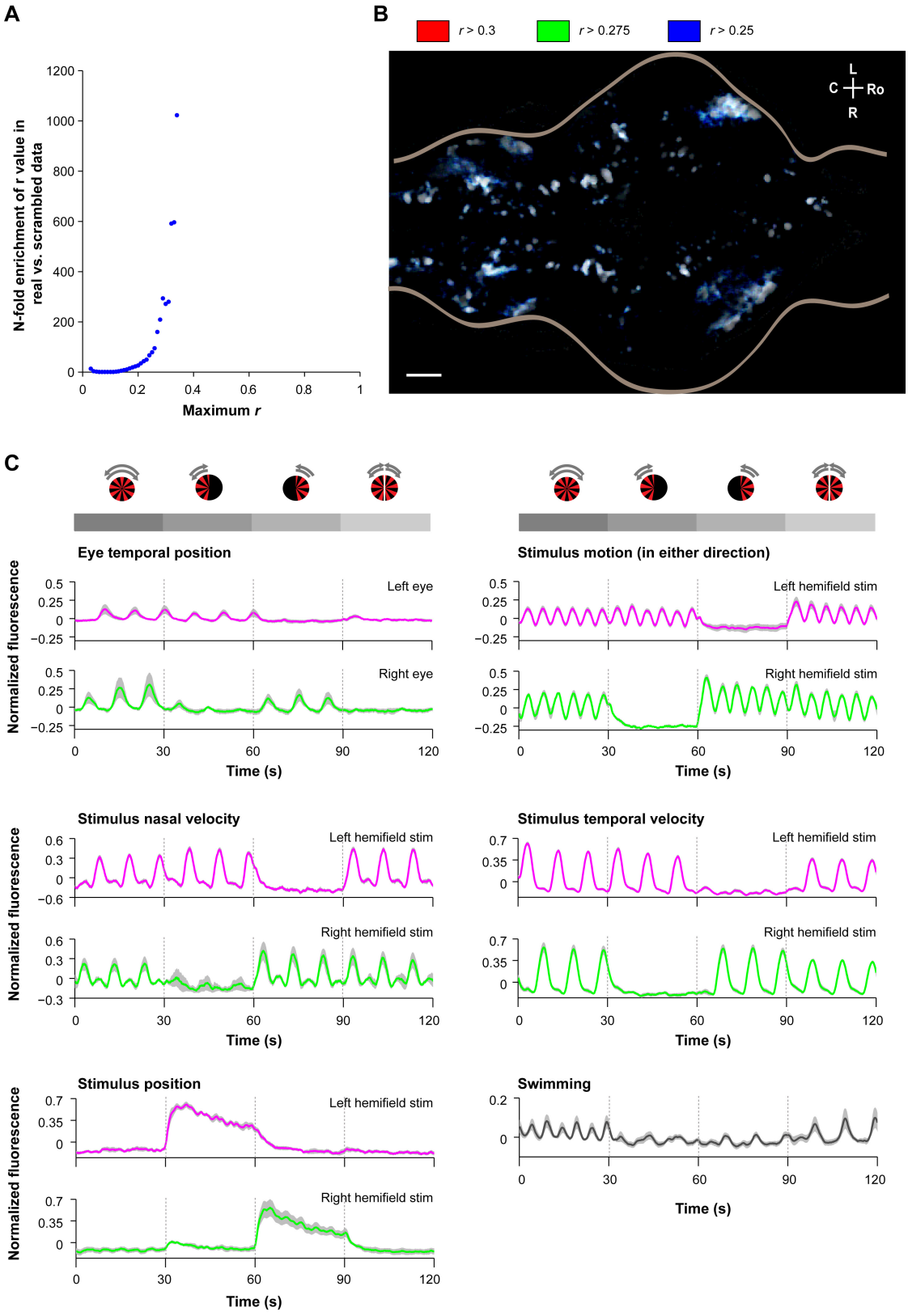

Figure S7
Portugues et al.

Figure S7. Threshold choice and traces for regressor maps (related to Figure 7)

(A) The N-fold enrichment of the maximum absolute regression coefficient (across all regressors) for every voxel in the real data compared to the equivalent computation performed using shuffled versions of the same regressors (8 second blocks; n=1,568,168 cube ROIs from 7 fish). The value of 0.3 is more than 200 times more common in the real data, indicating that this is a conservative threshold for selecting ROIs with activity correlated to the behavior.

(B) Z-projection of voxels with activity correlated to at least one regressor at three different thresholds: 0.25 in blue, 0.275 in green and 0.3 in red. The pattern of white areas with blue borders shows that reducing the threshold changes the boundaries of identified regions and contributes noise, but does not result in the identification of more active areas, and indicates that the map is robust to the precise choice of threshold. Scale bar is 50 microns.

(C) Average normalized fluorescence traces for the functional structures shown in Figure 7. All traces are the mean across fish with SEM shown by gray shading (n=6 fish). A schematic of the four stimuli is shown. Gray boxes and dotted lines indicate the duration of each of the four stimuli in all plots.

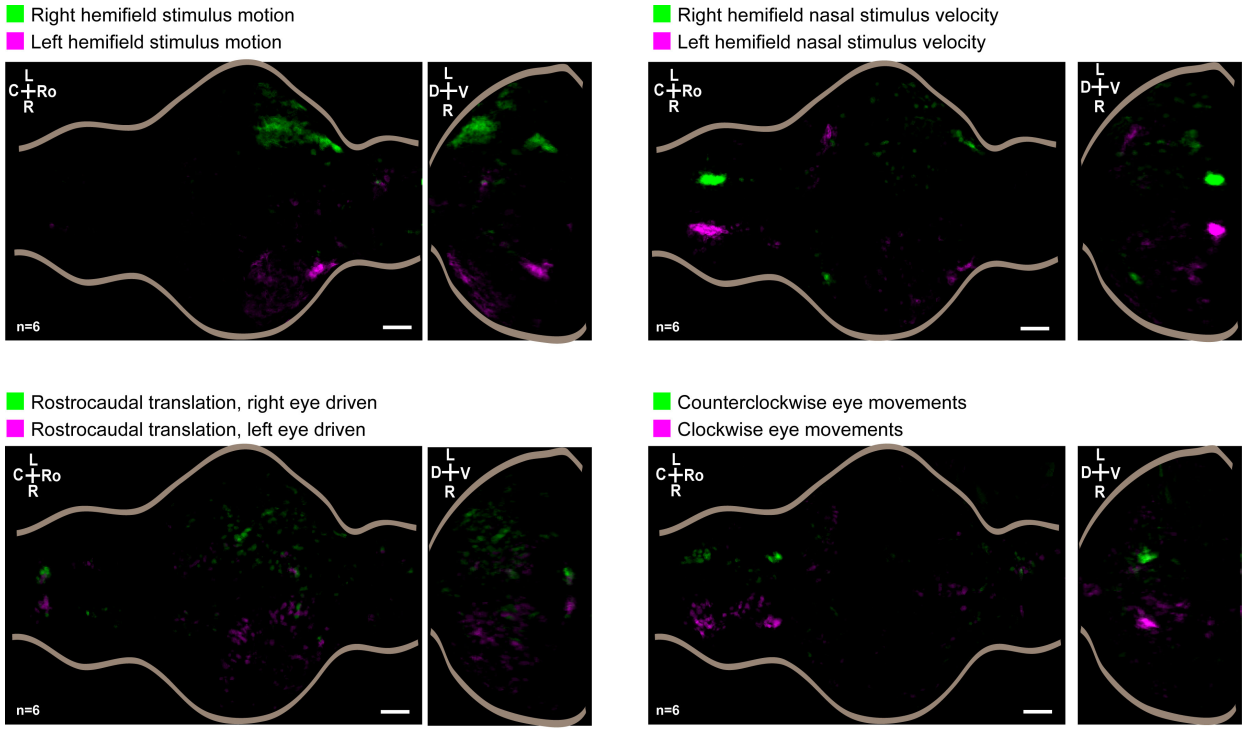

Figure S8
Portugues et al.

Figure S8. Clusters from Figure 8A (related to Figure 8)

We plot the eight clusters from Figure 8A in corresponding pairs for ease of viewing. Scale bars are 50 microns. Note that in the two upper panels, activity relates to stimulus motion in either the right or left hemifields, regardless of the stimulus on the opposite hemifield. In the left lower panel, on the other hand, activity in the two clusters results from integrating the stimuli in both hemifields. For instance, in the case of 'rostrocaudal translation, right eye driven', activity occurs when the right hemifield is presented with nasal to temporal (rostrocaudal) motion, but is suppressed when the left hemifield is simultaneously presented with temporal to nasal motion (i.e. during rotational motion).

Supplemental Movie Legends

Movie S1. **Robust OKR behavior**

Eye movements of a zebrafish larva can be tracked while it is imaged under a two-photon microscope. Red and black traces denote extracted position traces of the left and right eyes respectively.

Movie S2. Raw calcium data

Two planes of raw GCaMP5G imaging data are shown (averaged over 3 repetitions), at 100 and 145μm from the dorsal surface of the optic tectum. Amongst other activity, the left image shows direction selective calcium responses in different layers in the tectal neuropil and cells in the hindbrain which alternate with clockwise and anticlockwise stimulus. The plane on the right shows the moving eyes and relative stability of adjacent regions of the brain. Movies are 4 times real speed.

Movie S3. Activity dynamics in a single fish

The ROIs automatically identified in the brain of a single fish are color-coded as in Figure 1 (starting view is same field of view as in Figure 1C-dorsal). The analysis identifies both groups of cells and neuropil regions that are active, as well as many individual cell somas, most notably in the tectal stratum periventriculare and in the left habenula.

Movie S4. Annotated brain stack

We segmented the brain into 23 broad anatomical regions and display them here in different colors. The regions are:

- right/left optic tectum neuropil
- right/left habenula
- right/left optic tectum stratum periventriculare
- right/left pretectum / thalamus

- right/left cerebellum
- right/left rostral hindbrain
- right/left caudal hindbrain
- right/left rostral ventral hindbrain neuropil
- right/left caudal ventral hindbrain neuropil / inferior olive
- torus longitudinalis
- right/left other midbrain areas
- right/left other forebrain areas

Movie S5. ROIs across multiple fish reveal reliable activation of the same anatomical structures

The top, middle and bottom view show the ROIs of one, two and six brains that have been averaged to reveal consistently active structures across individuals. The color code and field of view is the same as in Figure 1C - dorsal.

Movie S6. Activity movie of average brain

Raw data from multiple individual fish are registered and summed before functional segmentation and analysis. A dorsal view of activity in ROIs segmented from data summed across three individual fish brains is shown in the middle panel (same field of view as Figure 1C - dorsal). Corresponding side views for the left and right sides of the brain are shown in the top and bottom panels respectively. The stimulus presented is shown on the top left. Activity in the brain follows the stimulus period except for some retinal ganglion arborization fields (including the tectum) which display activity at double the stimulus frequency. Movie is shown at 4 times speed.

Movie S7. Automatically detected ROIs in the average brain

The ROIs automatically identified using the raw data of three registered and averaged brains are color-coded as in Figure 1 (starting view is same field of view as in Figure 1C-dorsal).

Movie S8. Animation of average brain color map to show spatial gradients of activity phase

The phase map of ROIs segmented from the brain-averaged data in Figure 2G is displayed with a compressed color map to show variations in phase with high resolution. The previous 360˚ map is compressed to the 90˚ between maximum stimulus velocity and maximum position and repeated for both directions. The hsv color map is then rotated to make the spatial progression of response phase more apparent. Spatial gradients of response time appear as waves of color moving across the image. Dorsal and side views are shown as for Movie S7. In the top panel arrows show (from left to right) ventral hindbrain neuropil, dorsal hindbrain and cerebellum. In the middle panel arrows show (from left to right) top view of hindbrain, cerebellum and cells in the pretectum. The arrow in the bottom panel shows the cerebellum.

Movie S9. Diverging and converging stimulus

Bilateral converging/diverging whole field motion stimulation elicits convergence and divergence of the eyes. The temporal to nasal converging phase often also elicits an optomotor swim.

Movie S10. Three-dimensional anatomical location of clusters

Three-dimensional localization, averaged across 7 aligned fish brains, of the functional clusters shown in Figure 4B. Top: 8 bilaterally symmetric clusters. Colors legend in Figure 4B. Bottom: 5 pooled clusters with symmetric distribution, correlated with swimming activity.

Supplemental Experimental Procedures

Behavior tracking and analysis

Behavior tracking was performed with Matlab (Mathworks, USA). Tail angle was detected by manually selecting the point, in one image, at which the tail exited the

agarose, and then, for each image, automatically finding the line centered on this point along which pixel brightness was maximal. Bouts of swimming were detected by taking the rolling standard deviation of tail angle with a 15 ms window. Eye position was extracted by thresholding the image and fitting with an ellipse. In cases where image quality made fitting the eyes unreliable we used an alternative method to extract accurate eye angles. Principal component analysis was applied to the video frames to identify sets of pixels whose brightness changed with eye motion. The video data was projected onto the first two principal components, and eye angle was obtained by fitting the traces to a set of manual measurements of eye angle from representative frames, using a third-order polynomial. For correlation analysis, all of the processed behavior data was then resampled by linear interpolation to 5 times the effective calcium imaging frame rate (40 frames per second) to allow straightforward alignment with the functional data.

Automated ROI segmentation

Automatic segmentation of regions of interest (ROIs) was performed using the following iterative method. The first step involves finding voxels whose activity correlates closely with that of neighbouring ones. Therefore, for every voxel, the average correlation with the 124 surrounding voxels in a 5 x 5 x 5 cube was determined. The outcome of this procedure is a three dimensional anatomical stack of correlation values. The second step in the ROI determination procedure involves using these correlation values to grow ROIs. The first ROI is determined by choosing the voxel with the highest local correlation and using this as a "seed". This voxel has 6 closest neighbours (the voxels above, below, to the left, to the right, rostral and caudal to it). If the correlation of the activity in any of these neighbouring voxels with the activity in the "seed" voxel exceeded a threshold, the voxel was incorporated into the ROI. The procedure was then repeated iteratively by checking all the neighbours of all the voxels that comprise the current ROI estimate (once a new voxel is added, its neighbours need to be checked). On each iteration, a morphological close operation was performed to remove holes within ROIs (using Matlab imclose function). This operation causes a voxel which does not currently belong to an ROI, but all of whose neighbors do, to be incorporated into the ROI. Once no more voxels are added, the ROI is considered segmented and we proceed to find the voxel with

the next highest local correlation value in the 3D stack of correlation values and use that as the "seed" for the next ROI. Threshold values were chosen by the experimenter based on manual inspection of the ROIs produced, and then applied uniformly to all fish from the same experimental group. ROIs smaller than 50 voxels were eliminated, and the process was repeated until seeded ROIs would no longer grow past this limit. While some ROIs appear to align with single cell bodies, larger ROIs encompassing several cells are also produced. To reduce the chance that variation of activity between nearby cells is lost by averaging together their signals, all ROIs were split into units of approximately the size of one cell body (300 voxels) by iterative bisection along their longest axis. Since the eyes are moving in these experiments, this method will tend to also find ROIs that localize to the eyes or autofluorescent skin around the eyes which undergoes deformation during eye movements and other regions of sharp transition in brightness around moving parts of the fish. We applied spheroidal masks, fit by hand, to first remove the eyes from the imaging data, and, following segmentation, ROIs localized to the skin surface were removed manually.